

LP-BFGS ATTACK: AN ADVERSARIAL ATTACK BASED ON THE HESSIAN WITH LIMITED PIXELS

Jiebao Zhang¹, Wenhua Qian^{1*}, Rencan Nie¹, Jinde Cao², Dan Xu¹

¹School of Information Science and Engineering, Yunnan University, Kunming 650500, China

²School of Mathematics, Southeast University, Nanjing 210096, China

ABSTRACT

Deep neural networks are vulnerable to adversarial attacks. Most white-box attacks are based on the gradient of models to the input. Since the computation and memory budget, adversarial attacks based on the Hessian information are not paid enough attention. In this work, we study the attack performance and computation cost of the attack method based on the Hessian with a limited perturbation pixel number. Specifically, we propose the Limited Pixel BFGS (LP-BFGS) attack method by incorporating the BFGS algorithm. Some pixels are selected as perturbation pixels by the Integrated Gradient algorithm, which are regarded as optimization variables of the LP-BFGS attack. Experimental results across different networks and datasets with various perturbation pixel numbers demonstrate our approach has a comparable attack with an acceptable computation compared with existing solutions.

Index Terms— Adversarial examples, adversarial attacks, deep neural networks, BFGS method

1. INTRODUCTION

Deep Neural Networks (DNNs) have surpassing performance on the image classification task [1]. However, researchers have found that DNNs are highly susceptible to small malicious perturbations crafted by adversaries [2, 3]. Specifically, malicious perturbations in original examples can significantly harm the performance of DNNs. DNNs are therefore untrustworthy for security-sensitive tasks. Many adversarial attack methods have been proposed to seek perturbations according to the unique properties of DNNs and optimization techniques.

Depending on the attacker’s knowledge of the target model, adversarial attacks can be divided into two categories:

white-box attacks and black-box attacks. White-box attacks assume that attackers have detailed information about the target model (*e.g.*, the model structure, training data, and model weight), and they can be further classified into optimization-based attacks [2, 3, 4], single-step attacks [5, 6], and iterative attacks [7, 8, 9, 10]. Optimization-based attacks formulate finding the optimal perturbation as a box-constrained optimization problem. The L-BFGS attack uses the Limited-Memory BFGS method to solve the box-constrained problem [3]. Compared with the L-BFGS attack, the C&W [4] attack uses variable substitution to bypass the box constraint and uses a more efficient objective function. Furthermore, it uses the Adam optimizer [11] to find the optimal perturbation. Single-step attacks are simple and efficient and can alleviate the high computation cost caused by optimization-based attacks. Since the model is assumed to be locally linear, perturbations in single-step attacks are added directly along the gradient [5, 6]. Iterative attacks add perturbations in multiple steps, achieving a tradeoff between the computation and the attack performance. Black-box attacks mean that attackers have little information about the structure and parameters of the target model. Compared with white-box attacks, they also can achieve an equivalent attack by querying the output (*e.g.*, the confidence score or final decision) of the model [12, 13, 14].

Generating adversarial examples can be seen as the inverse process of training a model (*i.e.*, the loss maximization vs. the loss minimization). Besides, the demand that perturbations are not imperceptible to human eyes mitigates the dimension of the optimization variable. Recent white-box attacks have primarily focused on the usage of gradient information. Since the computation cost and memory limitation derived from the Hessian, the attacks utilizing the Hessian or approximate Hessian are gradually shelved. In this paper, to investigate the attack performance and time cost of methods utilizing the Hessian information, we put forward the Limited Pixel BFGS attack (LP-BFGS) method inspired by the quasi-Newton optimizer (*i.e.*, the BFGS method). Concretely, for an image, we use the Integrated Gradient algorithm to compute the attribution score of pixels for the label. Some pixels with the highest attribution score are selected as the perturbation pixels, which naturally reduce the dimension of the opti-

* Corresponding author: Wenhua Qian. Email: whqian@ynu.edu.cn.

This work was supported by the Research Foundation of Yunnan Province No.202002AD08001, 202001BB050043, 2019FA044, National Natural Science Foundation of China under Grants No.62162065, Provincial Foundation for Leaders of Disciplines in Science and Technology No.2019HB121, in part by the Postgraduate Research and Innovation Foundation of Yunnan University (No.2021Y281, No.2021Z078), and in part by the Postgraduate Practice and Innovation Foundation of Yunnan University (No.2021Y179, No.2021Y171).

mization variable. The main contributions of this work are as follows:

- We propose a LP-BFGS attack method with the guidance of the Hessian, which only perturbs some pixels.
- We investigate the effect of loss functions and perturbation pixel numbers on the performance of the LP-BFGS attack.
- We conduct experiments across various datasets and models to verify that the LP-BFGS attack can achieve a comparable attack with an acceptable computation cost.

2. METHOD

2.1. Problem Formulation

An image with the channel C , height H and width W , is denoted as a vector $x \in R^{C \times H \times W}$, and the corresponding label is \bar{y} . A deep neural network M -classifier can be regarded as a function $g : R^{C \times H \times W} \rightarrow R^M$. The prediction of g for the image x is $\arg \max_i g(x)_i$. Given the distance function $d(\cdot, \cdot)$ and $\varepsilon > 0$, an adversarial example \hat{x} satisfies the following formula:

$$\arg \max_i g(\hat{x})_i \neq \bar{y}, \quad d(x, \hat{x}) \leq \varepsilon. \quad (1)$$

The adversarial attack is to deal with the intractable problem (1) and seek the adversarial example. In general, the objective function in (1) is relaxed to maximize the training loss L (i.e., the cross-entropy loss), and the distance function is the Euclidean distance. The adversarial attack can be formulated as follows:

$$\max L(g(\hat{x}), \bar{y}) \quad \text{s.t.} \quad \|\hat{x} - x\| \leq \varepsilon. \quad (2)$$

2.2. Pixel Selector

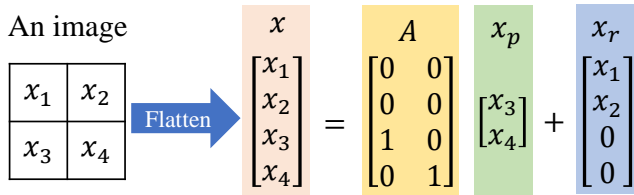


Fig. 1: The illustration that a 2×2 image endures procedures described in Section 2.2. x_3 and x_4 are selected as the perturbation pixel.

Current adversarial attack methods usually perturb all pixels of an image. In this work, we limit the number of pixels that can be perturbed according to the magnitude of the attribution score of pixels with respect to the final decision. Concretely, for an image x , we use Integrated Gradients algorithms [15] to assign attribution scores to each pixel with

respect to the label \bar{y} . Afterwards, K pixels whose attribution scores are top- K are selected as perturbation pixels, denoted as a vector $x_p \in R^K$, $K \ll C \times H \times W$. Because the size of the vectors x and x_p is inconsistent, we use the matrix A to raise the dimension of x_p , making x and x_p are consistent. To some extent, the matrix A records the position map between x_p and x , as shown in Fig. 1. When the pixels that can be perturbed in the original image x are removed, the remaining pixels with fixed values are recorded as $x_r \in R^{C \times H \times W}$. Then we have the following formula:

$$x = Ax_p + x_r. \quad (3)$$

2.3. Limited Pixel BFGS Attack

Algorithm 1 Limited Pixel BFGS Attack

Input: An image x , the corresponding label \bar{y} , and the loss function $L(w_p, x, \bar{y})$.

Input: The convergence tolerance $\epsilon > 0$, iteration $T > 0$.

Output: An adversarial image \hat{x} .

- 1: Obtain A , x_p , and x_r by the procedure described in Section 2.2
 - 2: $k = 0$
 - 3: $w_p^k = \text{atanh}(2x_p - 1)$, $H^k = I$
 - 4: **while** $\|\nabla_{w_p} L^k\| > \epsilon$ **or** $k < T$ **do**
 - 5: $d^k = -H^k \nabla_{w_p} L^k$
 - 6: $w_p^{k+1} = w_p^k + \alpha^k d^k$ where α^k satisfies the Wolfe condition.
 - 7: $s^k = w_p^{k+1} - w_p^k$
 - 8: $y^k = \nabla_{w_p} L^{k+1} - \nabla_{w_p} L^k$
 - 9: Compute H^{k+1} by (10)
 - 10: $k = k + 1$
 - 11: **end while**
 - 12: $\hat{w}_p = w_p^k$
 - 13: Obtain the adversarial image \hat{x} by (13)
 - 14: **return** \hat{x}
-

General BFGS Method. For the objective function $f(x)$, Newton methods use the Taylor series to make a second-order approximation of the function at the current iterate x^k and solve it:

$$m^k(p) = f^k + \nabla(f^k)^T p + \frac{1}{2} p^T B^k p, \quad (4)$$

where $m^k(p)$ denotes the approximation function, $f^k = f(x^k)$, and B^k is an $n \times n$ symmetric positive definite matrix. The search direction d^k is:

$$d^k = -(B^k)^{-1} \nabla f^k, \quad (5)$$

and the new iteration is:

$$x^{k+1} = x^k + \alpha^k d^k, \quad (6)$$

where α^k denotes the step length. Notably, the computation and memory costs of the Hessian matrix in the optimization are considerable, while the variable has a large size.

Instead of computing the Hessian, the popular quasi-Newton method, the BFGS method, revises the approximate Hessian B^k (or inverse Hessian H^k) in k -th iteration by the most recently observed information about the objective function [16]. To make the approximate Hessian as close as possible to the real Hessian, the approximate Hessian B^k should satisfy the *secant equation*:

$$B^{k+1} s^k = y^k, \quad (7)$$

where $s^k = x^{k+1} - x^k$ and $y^k = \nabla f^{k+1} - \nabla f^k$. By premultiplying (7) by s^k , we have $(s^k)^T B^{k+1} s^k = (s^k)^T y^k$. B^{k+1} is positive definite, we have:

$$(s^k)^T y^k > 0, \quad (8)$$

which is *curvature condition*. In nonconvex functions, the curvature condition is guaranteed by imposing the Wolfe condition on the line search. The common update strategy of B^{k+1} is as follows:

$$B^{k+1} = \left(I - \rho^k y^k (s^k)^T \right) B^k \left(I - \rho^k s^k (y^k)^T \right) + \rho^k y^k (y^k)^T, \quad (9)$$

where $\rho_k = \frac{1}{(y^k)^T s^k}$. Moreover, to alleviate the computation of solving equations in (5), the inverse Hessian approximation H^k is updated as follows:

$$H^{k+1} = \left(I - \rho^k s^k (y^k)^T \right) H^k \left(I - \rho^k y^k (s^k)^T \right) + \rho^k s^k (s^k)^T. \quad (10)$$

Limited Pixel BFGS Attack. In Section 2.1, the adversarial attack is formulated as an optimization problem with a constraint. In [3], the adversarial attack is formulated as a box-constrained problem. In the following study, the adversarial attack is reformulated as an unconstrained problem by the variable substitution [4]. In this paper, we absorb the pioneers' scheme and incorporate the pixel selector mentioned in Section 2.2. We propose the LP-BFGS method as a novel adversarial attack. It introduces a new variable $w_p \in (-\infty, +\infty)^K$ to bypass the constraint $x_p \in [0, 1]^K$:

$$w_p = \text{atanh}(2x_p - 1). \quad (11)$$

In this way, we convert the optimization problem with the variable x into the one with the variable w_p , dramatically reducing the optimization variable's dimension and relieving the computation burden and memory consumption. This proposed strategy also bypasses the box constraint. So we can solve the unconstrained optimization problem to find optimal adversarial examples by the BFGS optimizer:

$$\hat{w}_p = \min_{w_p} L(w_p, x, \bar{y}), \quad (12)$$

where the optimization result is \hat{w}_p . The proposed scheme is summarized in Algorithm 1. The corresponding adversarial image would be reconstructed by:

$$\hat{x} = R(\hat{w}_p) = A \left(\frac{1}{2} (\tanh(\hat{w}_p) + 1) \right) + x_r. \quad (13)$$

Moreover, we present three objective functions of the LP-

BFGS attack, which are mostly the same except for the \hat{L} :

$$L = \|R(w_p) - x\| + c \cdot \hat{L}. \quad (14)$$

There are three kinds of formulas of \hat{L} :

$$\hat{L} = -(-\log \bar{Z}(w_p)_{\bar{y}}), \quad (15)$$

$$\hat{L} = \max \{ \max \{ Z(w_p)_{\bar{y}} - Z(w_p)_{i, i \neq \bar{y}} \}, -\kappa \}, \quad (16)$$

$$\hat{L} = \max \{ \max \{ \log \bar{Z}(w_p)_{\bar{y}} - \log \bar{Z}(w_p)_{i, i \neq \bar{y}} \}, -\kappa \}, \quad (17)$$

where $Z(w_p)_i = g(R(\hat{w}_p))_i$, $\bar{Z}(w_p)_i = \text{softmax}(g(R(\hat{w}_p)))_i$, the constant c implicitly controls the balance between the perturbation magnitude and the rest loss, and $\kappa \geq 0$ is a hyperparameter for the attack transferability.

3. EXPERIMENTS

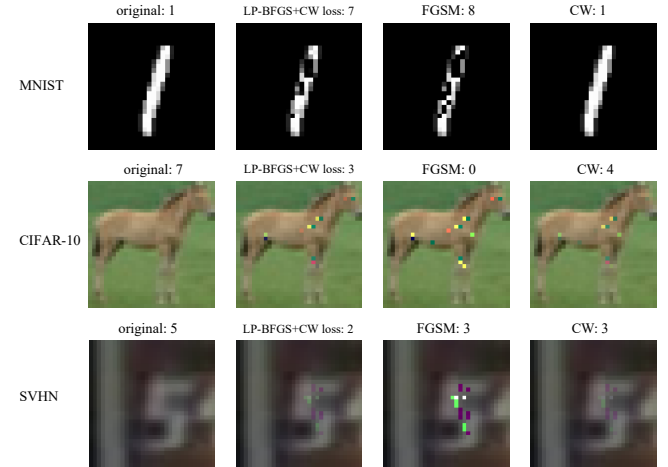


Fig. 2: Some adversarial examples generated by three attack methods with the perturbation pixel number $K = 20$. The title on each image is the label given by the target model.

Datasets and models. We conduct extensive experiments on the MNIST [17], CIFAR-10 [18], and SVHN [19] ¹. The corresponding models trained on them are FC-256-128, Res-20 [20], and Res-20.

Attack methods and metrics. The FGSM [5] and C&W [4] are adopted for the performance comparison. All attack methods will limit the perturbation pixel number for a fair comparison. For the FGSM, the L_∞ norm of the perturbation equals 1.0. For the C&W and LP-BFGS attack, the constant c is set to 1e3, and the iteration $T = 200$. The step size of the Adam optimizer in the C&W is set to 0.1. Unless otherwise specified, 1000 images are randomly sampled from the test set in each evaluation. Besides the attack success rate (ASR) and confidence score, the L_1 , L_2 , and L_∞ of the perturbation are also recorded.

¹The code of LP-BFGS attack is available at <https://github.com/wowotou1998/LP-BFGS-attack>.

Table 1: The comparison of the attack performance across various models and datasets with different perturbation pixel numbers.

Pixel Num	Attack	MNIST					CIFAR-10					SVHN				
		ASR(%)	Confidence score	L_1	L_2	L_∞	ASR(%)	Confidence score	L_1	L_2	L_∞	ASR(%)	Confidence score	L_1	L_2	L_∞
$k = 5$	LP-BFGS+CW loss	6.73	0.51	3.12	1.60	0.92	20.04	0.43	0.76	0.40	0.29	11.85	0.39	1.02	0.50	0.32
	FGSM	7.14	0.71	4.63	2.11	0.99	13.33	0.67	2.66	1.30	0.77	9.91	0.53	2.57	1.18	0.64
	C&W	3.98	0.48	2.49	1.17	0.61	18.14	0.44	0.52	0.26	0.17	10.02	0.39	0.75	0.35	0.19
$k = 10$	LP-BFGS+CW loss	18.76	0.49	4.91	1.93	0.91	34.73	0.43	1.64	0.63	0.35	21.90	0.39	2.15	0.77	0.40
	FGSM	19.79	0.73	8.45	2.82	1.00	18.78	0.70	5.22	1.80	0.80	13.83	0.58	5.26	1.72	0.70
	C&W	12.27	0.48	4.33	1.50	0.64	31.11	0.46	1.08	0.39	0.20	19.83	0.41	1.63	0.56	0.26
$k = 15$	LP-BFGS+CW loss	30.11	0.48	7.23	2.35	0.93	47.77	0.43	2.38	0.76	0.38	35.96	0.40	3.18	0.94	0.40
	FGSM	32.04	0.71	12.56	3.44	1.00	22.05	0.68	7.64	2.18	0.84	20.84	0.58	7.73	2.09	0.72
	C&W	19.23	0.47	6.24	1.81	0.65	43.10	0.45	1.48	0.45	0.21	34.23	0.42	2.31	0.66	0.26
$k = 20$	LP-BFGS+CW loss	48.01	0.47	9.31	2.67	0.95	58.47	0.44	2.69	0.75	0.36	43.59	0.40	4.05	1.04	0.42
	FGSM	52.29	0.70	16.46	3.93	1.00	26.36	0.70	10.32	2.54	0.84	25.19	0.57	10.27	2.40	0.73
	C&W	34.56	0.47	8.47	2.16	0.69	54.60	0.47	1.82	0.48	0.20	43.70	0.43	2.97	0.74	0.27

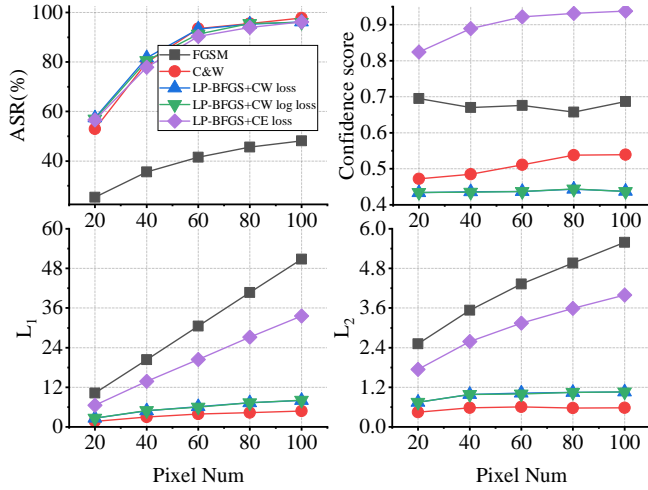


Fig. 3: The performance comparison with various perturbation pixel numbers.

Performance comparison. From Table 1, experimental results show that the LP-BFGS attack has a higher ASR than the advanced method C&W attack in most cases. It also has a lower perturbation magnitude and higher confidence score. Since we restrict only the L_∞ norm of perturbations in the FGSM, it outperforms the CW and LP-BFGS attack on some datasets when the perturbation pixel number $k = 5$, but at the cost of the considerable L_1 norm of perturbations, which is shown in Fig. 2. This method is not very effective in complex situations. For example, in the CIFAR-10 datasets, the ASR of the FGSM is only half that of the LP-BFGS attack while perturbation pixel number $k = 20$.

Loss function and perturbation pixel number. We also conduct some experiments to investigate the effect of the loss function and perturbation pixel number. 500 images are randomly sampled from the test set in each experiment. Three loss functions are evaluated, which are expressed in (16), (17), and (15). They are denoted by the CW loss, CW log loss, and

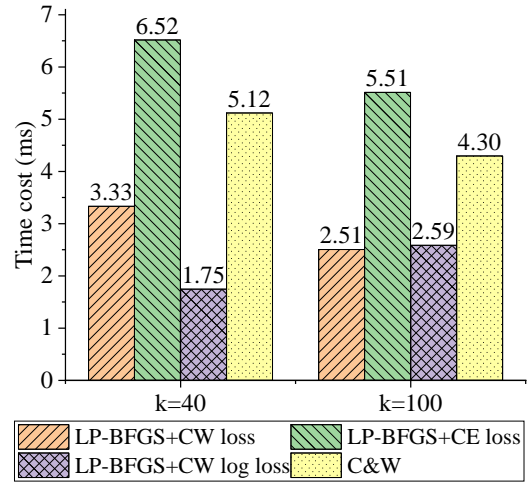


Fig. 4: The time cost comparison with the perturbation pixel number $k = 40$ and $k = 100$.

CE loss, respectively. From Fig. 3, we can see that with the increase of the pixel number, the performance of the BFGS attack family shows a slight disadvantage in contrast with the one of the C&W attack. But BFGS attacks have a comparable perturbation magnitude. Furthermore, as shown in Fig. 5, the BFGS attack family generally has a lower time cost than the C&W attack.

4. CONCLUSION

In this work, we propose the LP-BFGS attack method based on the Hessian with limited perturbation pixels. We explore the performance of the proposed method from various aspects. Experimental results demonstrate our approach's superior performance compared with existing solutions. There is room for improvement to increase the attack effect and time cost. The selection of pixels, the design of loss functions, and the usage of the optimization method are all worth exploring. Our study suggests avenues for future work.

5. REFERENCES

- [1] Waseem Rawat and Zenghui Wang, “Deep Convolutional Neural Networks for Image Classification: A Comprehensive Review,” *Neural Computation*, vol. 29, no. 9, pp. 2352–2449, 2017.
- [2] Battista Biggio, Iginio Corona, Davide Maiorca, Blaine Nelson, Nedim Srndic, Pavel Laskov, Giorgio Giacinto, and Fabio Roli, “Evasion attacks against machine learning at test time,” *CoRR*, vol. abs/1708.06131, 2017.
- [3] Christian Szegedy, Wojciech Zaremba, Ilya Sutskever, Joan Bruna, Dumitru Erhan, Ian J. Goodfellow, and Rob Fergus, “Intriguing properties of neural networks,” in *International Conference on Learning Representations*, 2014.
- [4] Nicholas Carlini and David A. Wagner, “Towards evaluating the robustness of neural networks,” in *Proceedings of the IEEE Symposium on Security and Privacy*, 2017, pp. 39–57.
- [5] Ian J. Goodfellow, Jonathon Shlens, and Christian Szegedy, “Explaining and harnessing adversarial examples,” in *International Conference on Learning Representations*, 2015.
- [6] Florian Tramèr, Alexey Kurakin, Nicolas Papernot, Ian J. Goodfellow, Dan Boneh, and Patrick D. McDaniel, “Ensemble adversarial training: Attacks and defenses,” in *International Conference on Learning Representations*, 2018.
- [7] Aleksander Madry, Aleksandar Makelov, Ludwig Schmidt, Dimitris Tsipras, and Adrian Vladu, “Towards deep learning models resistant to adversarial attacks,” in *International Conference on Learning Representations*, 2018.
- [8] Alexey Kurakin, Ian J. Goodfellow, and Samy Bengio, “Adversarial examples in the physical world,” *CoRR*, vol. abs/1607.02533, 2016.
- [9] Yinpeng Dong, Fangzhou Liao, Tianyu Pang, Hang Su, Jun Zhu, Xiaolin Hu, and Jianguo Li, “Boosting adversarial attacks with momentum,” in *Proceedings of the IEEE Conference on Computer Vision and Pattern Recognition*, 2018, pp. 9185–9193.
- [10] Seyed-Mohsen Moosavi-Dezfooli, Alhussein Fawzi, Omar Fawzi, and Pascal Frossard, “Universal adversarial perturbations,” *CoRR*, vol. abs/1610.08401, 2016.
- [11] Diederik P. Kingma and Jimmy Ba, “Adam: A method for stochastic optimization,” in *International Conference on Learning Representations*, 2015.
- [12] Jiawei Su, Danilo Vasconcellos Vargas, and Kouichi Sakurai, “One pixel attack for fooling deep neural networks,” *IEEE Transactions on Evolutionary Computation*, vol. 23, no. 5, pp. 828–841, 2019.
- [13] Pin-Yu Chen, Huan Zhang, Yash Sharma, Jinfeng Yi, and Cho-Jui Hsieh, “ZOO: Zeroth order optimization based black-box attacks to deep neural networks without training substitute models,” in *Proceedings of the ACM Workshop on Artificial Intelligence and Security*, 2017, pp. 15–26.
- [14] Wieland Brendel, Jonas Rauber, and Matthias Bethge, “Decision-based adversarial attacks: Reliable attacks against black-box machine learning models,” in *International Conference on Learning Representations*, 2018.
- [15] Mukund Sundararajan, Ankur Taly, and Qiqi Yan, “Axiomatic attribution for deep networks,” in *Proceedings of the International Conference on Machine Learning*, 2017, vol. 70, pp. 3319–3328.
- [16] “Quasi-newton methods,” in *Numerical Optimization*, number 1431-8598, pp. 192–221. New York, NY, 1999.
- [17] Yann Lecun, Ligon Bottou, Yoshua Bengio, and Patrick Haffner, “Gradient-based learning applied to document recognition,” *Proceedings of the IEEE*, vol. 86, no. 11, pp. 2278–2323, 1998.
- [18] Alex Krizhevsky, “Learning multiple layers of features from tiny images,” 2009.
- [19] Yuval Netzer, Tao Wang, Adam Coates, Alessandro Bisaccho, Bo Wu, and Andrew Ng, “Reading digits in natural images with unsupervised feature learning,” in *NIPS Workshop on Deep Learning and Unsupervised Feature Learning*, Jan. 2011.
- [20] Kaiming He, Xiangyu Zhang, Shaoqing Ren, and Jian Sun, “Deep residual learning for image recognition,” in *Proceedings of the IEEE Conference on Computer Vision and Pattern Recognition*, 2016, pp. 770–778.